The Relative Variation of Relativistic Radiation Belt Acceleration and Loss During Storms

Samuel D. Walton[1], C. Forsyth[1], I. J. Rae[2], N. P. Meredith[3], J. K. Sandhu[2], M.-T. Walach[4], K. R. Murphy[5]

[1]Mullard Space Science Laboratory, University College London, Dorking, UK
[2]Department of Maths, Physics and Electrical Engineering, Northumbria University, Newcastle upon Tyne, UK
[3]British Antarctic Survey, Cambridge, UK
[4]Physics Department, Lancaster University, LA1 4YB, UK
[5]Self

UCL

1. Introduction

Earth's outer Van Allen radiation belt is a highly dynamic environment of extremely energetic electrons The overall intensity of the population is influenced by both trapped electron flux and bounce loss cone (BLC) flux causing subsequent precipitation. The relative contribution of each component is highly variable with time and far from fully understood. **We statistically examine how BLC flux varies relative to trapped flux over the course of a geomagnetic storm.**

Data are provided by SAMPEX/PET ~1.0-6.0 MeV instrument, spanning 1992 to 2004. SAMPEX operated in a near-circular orbit at ~600km, inclined at 82° with a 90-minute period. PET's wide, 58° field of view allows sampling of large portions of the BLC, whilst also capturing portions of trapped particles at different points along the orbit. The long-duration dataset allows us to distinguish BLC from trapped particle measurements and statistically compare them.

2. Separation of BLC and Trapped Flux

Using IGRF magnetic field values local to SAMPEX, we approximate the spacecraft's location within the field relative to the stable trapping region for electrons, as well as the size of the BLC. We then use spacecraft attitude data to determine the percentage of the 58° field of view that was observing particles in the BLC (**Figure 1(a)**) or trapped particles (**Figure 1(b)**). We find that PET observes:

- **100% BLC over Europe and the North Atlantic**
- **varying percentages of trapped flux (up to ~80%) in the South Atlantic anomaly (SAA) region and surrounding.**

For the BLC dataset, we simply use only times when 100% detector coverage is achieved. For the trapped dataset, we use all times where coverage is ≥30% and multiply by a correction factor to provide 100% coverage. We assume that the non-trapped flux is negligible.

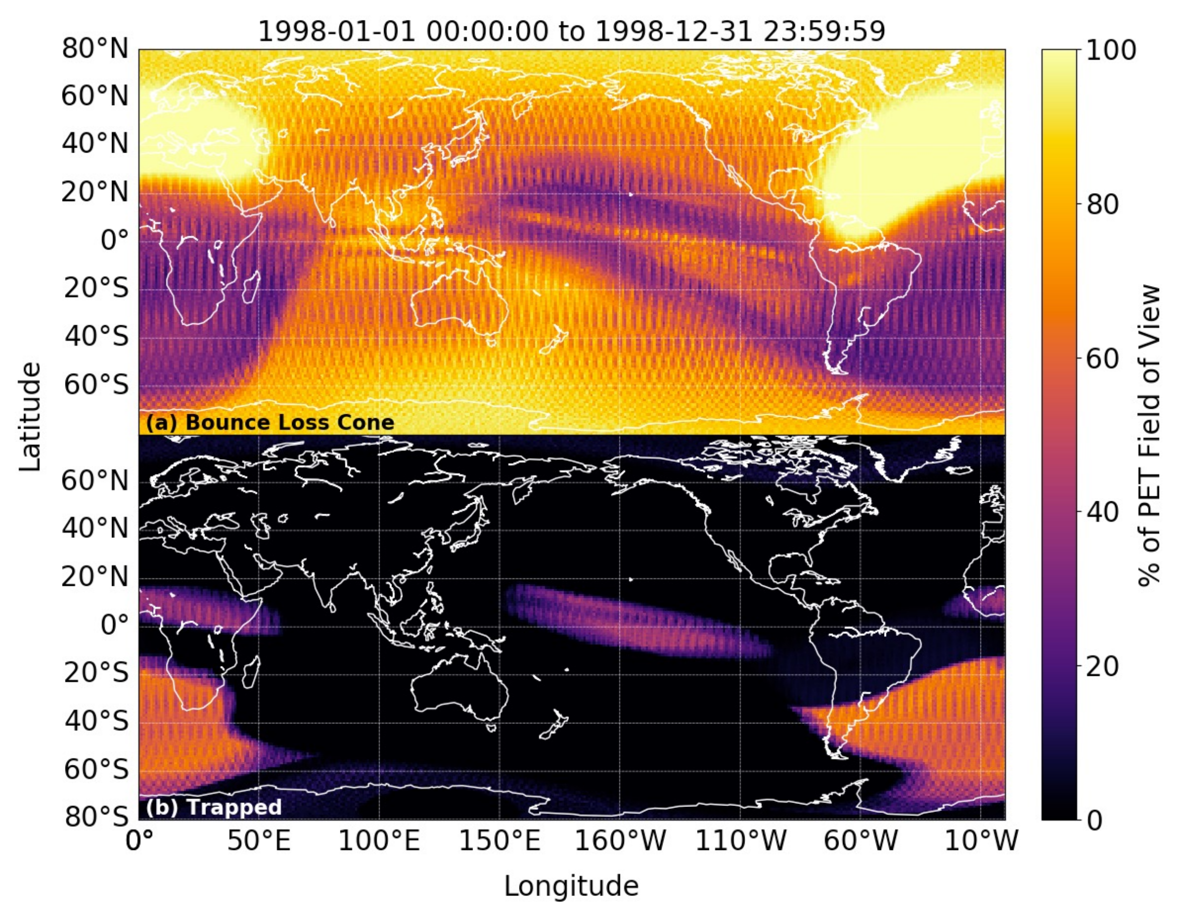

Figure 1: World maps showing the percentage of the SAMPEX/PET 58° field of view which was observing (a) flux in the bounce loss cone and (b) trapped flux for a particular 1x1° latitude-longitude bin. Mean values for the year of 1998 are shown.

samuel.walton.18@ucl.ac.uk

Acknowledgements
The authors would like to thank the SAMPEX and PET science teams for the data used in this study.

3a. SEA: Method

Figure 2 shows a superposed epoch analysis (SEA) performed using a method similar to *Murphy et al (2018)*. The 168 storms used are identified using the *Walach and Grocott (2019)* algorithm for the 1992-2004 period.

Individual storm periods are 'stretched' or 'compressed' in length to fit the normalised time axis shown, and the mean flux is calculated. Initial and main phases are grouped together and fitted from -20-0hrs relative to the epoch (minimum Sym-H). Recovery phases from 0-120hrs.

Figure 2(a) compares trapped and BLC fluxes during storms. **Figure 2(b)** examines changes in the BLC/trapped ratio, considering MLT quadrants separately to understand local time dependencies.

3b. SEA: Results

Figure 2(a) shows the 0-24 MLT SEA. We observe:

- **Enhanced relative loss outside plasmapause during main and early recovery phase.** Peak loss observed at maximum Sym-H.
- **Slight reduction in loss inside plasmapause**

Figure 2(b) shows Δratio for the 4 MLT quadrants. We observe:

- **Dawn-side (0-12hr) loss enhancement outside plasmapause.** More intense than Figure 2(a)
- **Post-noon (12-18hr) loss enhancement and fast drop-off thereafter**
- **Pre-midnight (18-24hr) enhancement at higher L-shell**

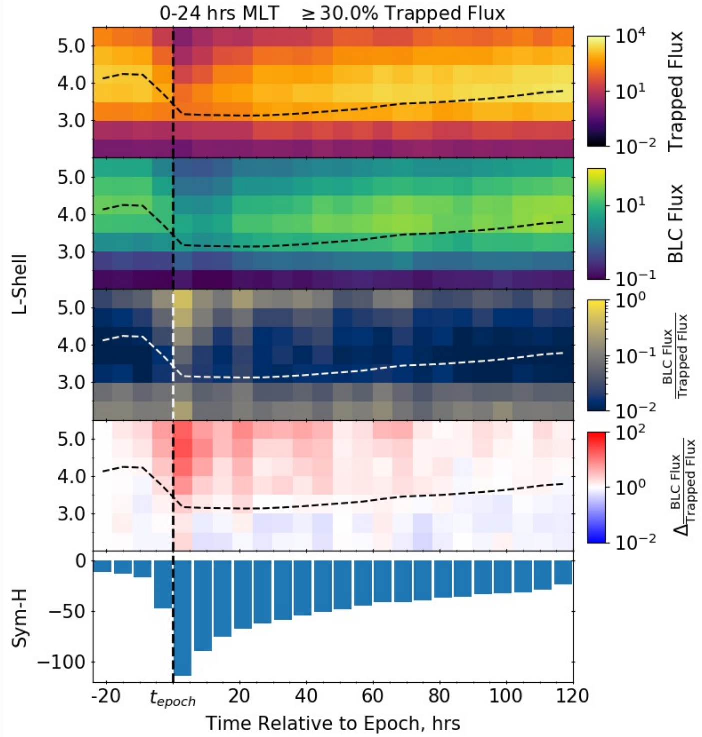

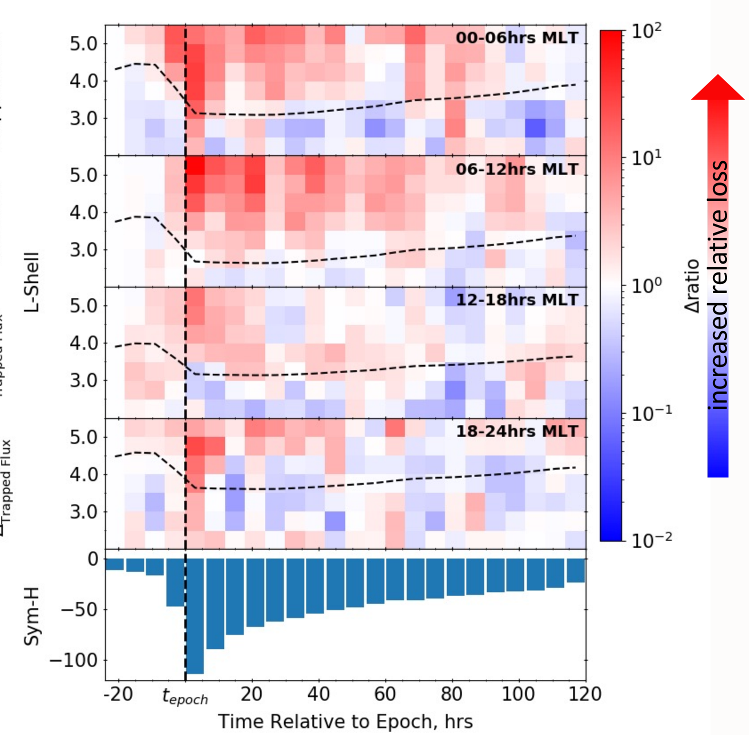

Figure 2(a): Superposed Epoch Analysis result along the normalised time axis. Panels show, from top to bottom; ~1-6 MeV electron flux, BLC flux, the ratio of BLC/trapped flux, the Δratio and Sym-H. Δratio indicates a change in the BLC/trapped ratio compared to the beginning of the storm. An increase in the ratio indicates and increase in BLC flux relative to trapped, or a relative enhancement in loss. The dashed black/white line indicates the *O'Brien and Moldwin (2003)* plasmapause model.

Figure 2(b): Superposed Epoch Analysis Δratio quantity (as explained in Figure 2(a) caption) broken down into all 4 MLT quadrants. Panels show, from top to bottom; 00-06hrs, 06-12hrs, 12-18hrs and 18-24hrs MLT,. The bottom panel shows Sym-H. The dashed line indicates the *O'Brien and Moldwin (2003)* plasmapause model. The vertical dashed line represents the epoch time at minimum Sym-H

References

1. Walach, M., & Grocott, A.(2019, jul).SuperDARN Observations During Geomagnetic Storms, Geomagnetically Active Times, and Enhanced Solar Wind Driving. JGR: Space Physics. doi: 10.1029/2019JA026816

2. Murphy, K. R., Watt, C. E. J., Mann, I. R., Jonathan Rae, I., Sibeck, D. G., Boyd, A. J., . . . Fennell, J.(2018, may). The Global Statistical Response of the Outer Radiation Belt During Geomagnetic Storms. GRL , doi: 10.1002/2017GL076674

3. O'Brien, T. P., & Moldwin, M. B. (2003, feb). Empirical plasmapause models from magnetic indices. GRL doi: 10.1029/2002GL016007

4. Meredith, N. P., J. Bortnik, R. B. Horne, W. Li, and X. -C. Shen (2021), Statistical investigation of the frequency dependence of the chorus source mechanism of plasmaspheric hiss. GRL. doi: 10.1002/2020GL092725.

5. Meredith, N. P., Horne, R. B., Kersten, T., Li, W., Bortnik, J., Sicard, A., & Yearby, K. H.(2018, jun).Global Model of Plasmaspheric Hiss From Multiple Satellite Observations. JGR: Space Physics doi: 10.1029/2018JA025226

samuel.walton.18@ucl.ac.uk

Acknowledgements

The authors would like to thank the SAMPEX and PET science teams for the data used in this study.

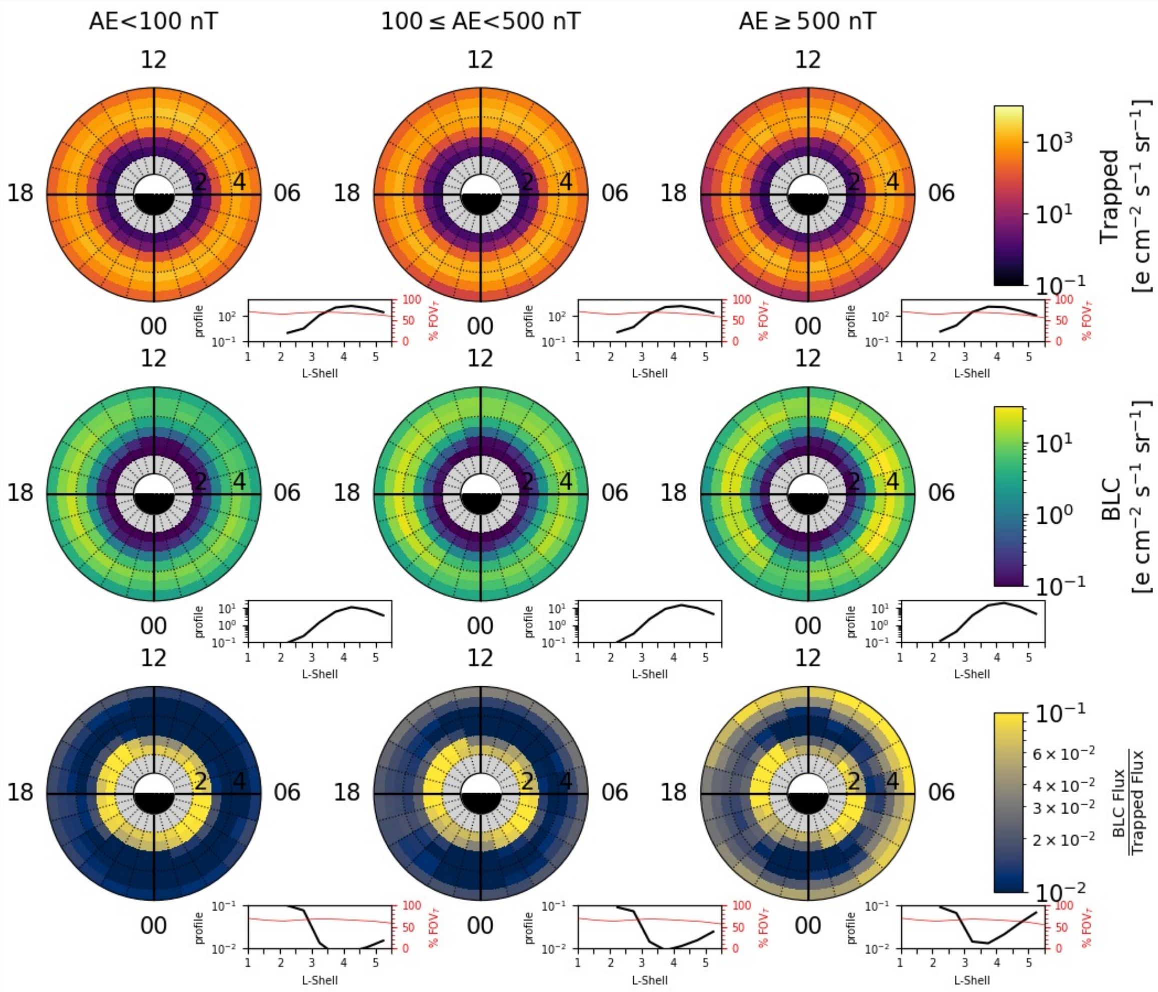

Figure 3: ~1-6 MeV electron flux from 1992-2004, parameterised by the AE index and displayed from 0-25 hrs MLT and L=2.0-5.5. L=1.0-2.0 is greyed due to the potential influence of proton contamination. Columns from left to right; low activity (AE<100 nT), medium-moderate activity (100<AE<500 nT) and high activity (AE>500 nT). Rows from top to bottom; trapped flux, BLC flux and BLC/trapped ratio. An increase in the ratio indicates enhanced loss relative to trapped flux. To the lower-right of each plot shows the radial profile of the quantity (black) and of the mean PET detector coverage (red).

4. L-MLT Variation with AE

Figure 3 shows spatial maps of the mean trapped (top row), BLC (middle row) and BLC/Trapped ratio (bottom row) fluxes for 1992-2004. Columns show parameterisation by the AE index, representing the level of geomagnetic disturbances as labelled. Mean radial profiles are shown to the lower right of the shown quantity (black) and PET detector percentage (red).
We observe, with increasing AE:

- **Reduced trapped flux intensity L≳5 from noon through morning sectors.**
- **Dawn-side enhancement in BLC flux L>3.5 by ~1 order of magnitude**
- **Predominantly dawn-side relative loss enhancement L>3.5 by ~1 order of magnitude. Enhancement of <1 order of magnitude from 14-22 MLT**

5. Discussion

We have analysed the relative contribution of MeV loss and acceleration during storms and periods of geomagnetic activity via a superposed epoch analysis and AE parameterisation.

- **Loss enhancement of ≳1 MeV electrons could indicate resonant scattering of particle pitch angles via magnetospheric waves, and subsequent precipitation into the atmosphere.**
- **Dawn-side storm-time is dominated by loss enhancement outside the plasmapause or L>3.5.** This is reminiscent of whistler-mode chorus wave signatures at mid-high latitudes *(Meredith et al 2021)* and indicates MeV electron precipitation following enhancement in wave power.
- **Weaker loss enhancement from 14-22 hrs MLT at all L-shell could be indicative of plasmaspheric hiss.** During storm time, this peaks around minimum Sym-H and rapidly reduces again. *Meredith et al (2018)* shows signatures of hiss close to this region.

samuel.walton.18@ucl.ac.uk

Acknowledgements
The authors would like to thank the SAMPEX and PET science teams for the data used in this study.